SAND2009-4628C

MESO-SCALE SIMULATION OF THE SHOCK COMPRESSION RESPONSE OF EQUIAXED AND NEEDLE MORPHOLOGY AL 6061-T6 POWDERS

D.A. Fredenburg[1], T.J. Vogler[2], N.N. Thadhani[1]

[1]Materials Science & Engineering, Georgia Institute of Technology, 771 Ferst Dr. Atlanta GA 30332
[2]Sandia National Laboratories, Livermore CA 94550

Abstract. With component sizes approaching the mesoscale, conventional size microstructures offer insufficient homogeneity in mechanical properties, forcing microstructures to be reduced to the nanoscale. This work examines the effect of a nanocrystalline surface layer on the dynamic consolidation response of two different morphology Al 6061-T6 powders. Shock-propagation through equiaxed and needle morphology Al 6061-T6 powder beds initially at 73.5 and 75.0 % theoretical density, respectively, is simulated at constant particle velocities ranging between 150 and 850 m/s. Shock velocity-particle velocity relationships are determined for powders both with and without the presence of a 2 μm high strength surface layer, which is representative of a nanocrystalline surface layer. Significant deviations in dynamic response are observed with the presence of the surface layer, especially at lower particle velocities. The equation of state (EOS) for both the homogeneous particles and those with a high strength surface layer are found to be best represented by a piecewise EOS.

Keywords: Al 6061-T6, meso-scale simulation, dynamic compaction, CTH.
PACS: 81.07.-b, 91.30.Mv, 81.20.Ev.

INTRODUCTION

Nanocrystalline aluminum alloys are attractive for numerous applications because they possess a high strength to weight ratio. However, as grain size decreases and strength increases, a corresponding decrease in ductility is also typically observed [1]. In an effort to increase ductility while maintaining strength, alloys have been produced with bi-modal grain structures composed of nano- and microcrystalline grains. Plane-strain machining techniques have been shown to produce particles with bi-modal grain structures, exhibiting microstructures that are nanocrystalline near the particle surface and microcrystalline in particle interiors [2]. Furthermore, shock-wave consolidation has been shown to successfully compact these powders into bulk forms while still retaining their original bimodal microstructures [3]. However, the effect of the high strength surface layers on the dynamic compaction response of these powders has not yet been explored.

Meso-scale simulations are extremely valuable for helping to understand phenomena which can not be probed experimentally, such as particle response to shock loading. Previous studies have shown qualitative agreement between 2-D simulated microstructures and recovered experimental microstructures, and serve to reinforce the validity of capturing accurate transient deformation characteristics through 2-D meso-scale simulations [4-6]. In this work, 2-D meso-scale simulations are employed to determine the effects of a high strength surface layer on the

dynamic compression response for two separate morphology powders.

EXPERIMENTAL PROCEDURE

Simulations are performed with CTH [7], utilizing 24 processors on a cluster at Sandia National Laboratories. Experimental microstructures of equiaxed and needle morphology powders are examined, and details of particles have been discussed elsewhere [2]. Initial density of the powder beds for the equiaxed and needle morphologies are 73.5 and 75.0% theoretical density, with the entire particle bed measuring 1.0 mm in width and 1.5 mm in the direction of stress propagation, which will henceforth be referred to as the y-direction.

The Al 6061-T6 particles are modeled using the Mie-Gruneisen EOS [7], and strength is described by the rate independent form of the Steinberg-Guinian-Lund (SGL) viscoplastic model with zero pressure yield strength (Y_0) equal to 0.29 GPa [8]. The effects of a high strength surface layer on the dynamic compaction characteristics is modeled by inserting a thin surface layer of approximately 2 μm along the particle perimeter with Y_0 equal to 0.5 GPa. This particular Y_0 is estimated through the yield relationship $\sigma_Y = H_V/3$, where σ_Y and H_V are the yield strength and Vickers hardness of the material, and correspond well with measured hardness values for 6061-T6 chips in the peak-aged condition formed through plane strain machining techniques [9]. A representative image of equiaxed particles with high strength surface layers is shown in Figure 1. Note that particles without the surface layer have the same outer boundary, but strength properties are homogeneous throughout the particle. Rectangular meshing is employed in the simulation, with sides measuring approximately 1.3 μm in length, such that the surface layer is represented by at most two cells along its inward normal.

Shock velocity (U_S)-particle velocity (u_P) relations for the powder configurations are determined by assigning a constant particle velocity to a rigid driver initially at y=0 which travels in the positive y direction. Shock velocity inside the powder mixture is determined by tracking the particle velocity through a series of tracer particles at known y-locations within the powder bed. Eight tracer particles are located at each of the y-locations 0.3, 0.6, 0.9, and 1.2 mm. By determining the arrival time of the travelling wave front at each of these y-locations, and knowing their relative separation distance, an estimate of the shock velocity in the powder can be obtained. The time at which the average particle velocity for tracers at each y-location reaches half of the assigned driver velocity is used to calculate the shock velocity in the powder.

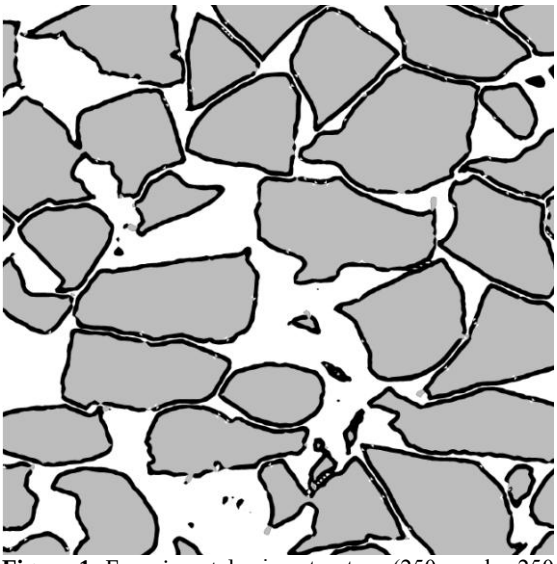

Figure 1. Experimental microstructure (250 μm by 250 μm) showing high strength surface layer (black) on equiaxed particles (gray).

RESULTS AND DISCUSSION

The simulated results illustrating the U_S-u_P relationships for both morphology powders with and without the high strength surface layer are shown in Figures 2 and 3. Particles with the high strength surface layer are denoted ‘with shell’. Error in calculated U_S is based on the standard deviation in velocity measured between the four series of tracer points, and is small compared to the scales shown in Figures 2 and 3.

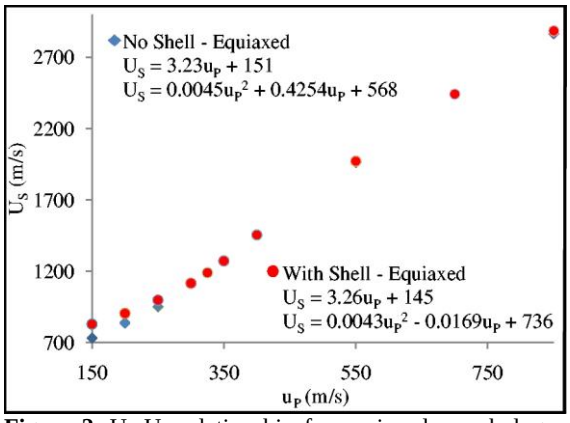

Figure 2. U_S-U_P relationship for equiaxed morphology particles with and without the presence of a high strength surface layer.

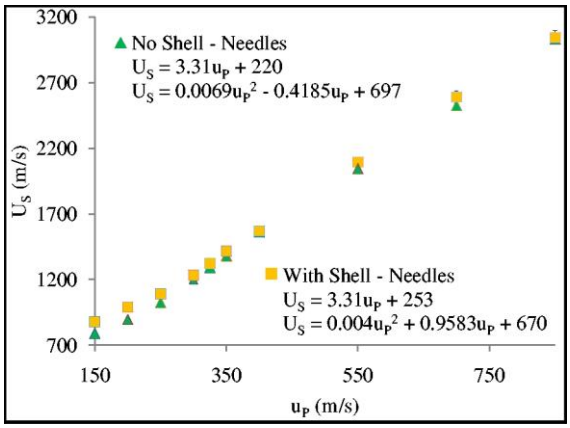

Figure 3. U_S-U_P relationship for needle morphology particles with and without the presence of a high strength surface layer.

Figures 2 and 3 illustrate that the presence of a high strength surface layer causes an increase in measured shock velocity for a given driver velocity. This is valid over the entire velocity range examined, with the exception of equiaxed particles at driver velocities of 325 and 350 m/s. Generally, larger increases in shock velocity are observed at lower assigned driver velocities. This can be explained if one envisions a snow plow pushing on two types of particles of the same size, one with a hard outer shell, and another softer particle with no shell. At lower velocities, the stresses transferred at particle contact points may be at or above the materials yield strength, and as the plow moves forward, the particles with the lower yield strength will compress more than the particles with the hard outer shell. Thus, increased deformation in the particles without the shell will result in a slower moving front, and a higher shock velocity will be observed in the particles with the shell. At higher velocities, the stresses should be well in excess of the materials yield strength and differences in shock velocity with the presence of a high strength surface shell should be minimal.

Investigating further the difference in shock velocity with the addition of a hard outer shell, the relative difference in U_S is plotted at each driver velocity. The difference decreases sharply with increasing driver velocity in the low velocity range before beginning to level off. The absolute minimum occurs at 325 and 400 m/s for the equiaxed and needles morphologies, and is attributed to a combination of strength and shape effects. Looking first at strength effects, the stress in the powder exceeds the dynamic yield of the high strength surface layer predicted by the SGL model [7] at velocities above 325 and 300 for the equiaxed and needle particles. For equiaxed particles, this transition to yield corresponds well with the observed minimum in shock velocity difference. In contrast, the needles transitions into yielding at lower driver velocities than where the observed absolute minimum in U_S difference occurs. However, a relative minimum is observed near a driver velocity of 300 m/s, and differences in the yielding behavior are attributed to differences in morphology whose effects are not fully understood.

The needle particles also exhibit a more pronounced increase in shock velocity for a given particle velocity over the entire velocity range investigated. This is attributed to the large aspect ratio of the needle particles, which results in a larger percentage of the particles being composed of the high strength material. The ratio of hard to soft material for the equiaxed and needles particles is found to be 0.195 and 0.270. The increase in the amount of hard surface material, in conjunction with morphological effects, is responsible for the decrease in deformation for the shelled needle particles and the observed increase in shock velocity.

In attempting to fit a single linear or quadratic equation to the observed U_S-u_P relationship for all powders, it is found that neither type of equation

accurately describes the observed behavior over the velocity range considered. The equations in Figures 3 and 4 give the best fit results for the observed U_S-u_P relationships over specific ranges of particle velocity. It is found that a quadratic relationship describes well the U_S-u_P relationship at particle velocities up to 300 m/s, and that a linear relationship is better suited for particle velocities 300 m/s and above. Note that the linear and quadratic equations shown in Figures 3 and 4 are only valid for the particle velocity ranges listed above, resulting in a piecewise EOS. An example of the linear and quadratic fits to the equiaxed particle data with the high strength surface shell is shown in Figure 5.

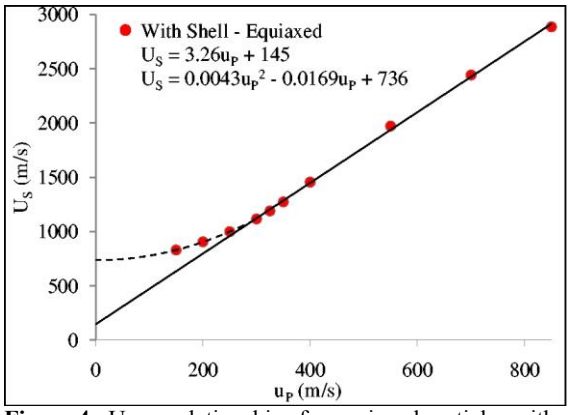

Figure 4. U_S-u_P relationships for equiaxed particles with shell, best fit quadratic (150-300 m/s) and linear (300-850 m/s) relations are shown.

The data suggest that there are certain particle velocity ranges over which even porous materials may be well described by linear equations of state, similar in form to that of solid materials.

CONCLUSIONS

Effects of particle morphology and the presence of high-strength surface layers on the shock compression response of Al 6061-T6 powders have been studied. The U_S-u_P relationship is found to be best described by a piecewise EOS, with a transition from quadratic to linear fit at 300 m/s. This suggests that porous materials, similar to their solid counterparts, can be described by linear equations of state under certain dynamic conditions. This result could considerably simplify continuum level simulations and experimental design for numerous powder compaction problems. Also, the relative difference in shock velocity at a given driver velocity can not be attributed solely to the increased strength of the outer shell, particle morphology also plays a role and is at present not fully understood.

ACKNOWLEDGEMENTS

Funding for this research was provided by the Laboratory Directed Research and Development Program of Sandia National Laboratories, a multiprogram laboratory operated by Sandia Corporation, a Lockheed Martin Company, for the United States Department of Energy's National Nuclear Security Administration under Contract DE-AC04-94AL85000.

REFERENCES

1. Han, B.Q., Ye, J., Tang, F., Schoenung, J., Lavernia, E.J., J. Mater. Sci. 42 (2007) 1660-1672.
2. Fredenburg, D.A., Vogler, T.J., Saldana, C.J., and Thadhani, N.N., "Shock consolidation of nanocrystalline aluminum for bulk component formation", in Shock Compression of Condensed Matter, 2007 (M. Elert, M.D. Furnish, R. Chau, N. Holmes, J. Nguyen, eds.), pp.1029-1032.
3. .Fredenburg, D.A., Vogler, T.J., Thadhani, N.N., Mater. Sci. Engr. A, submitted July 2009.
4. Meyers, M.A., Benson, D.J., and Olevsky, E.A., Acta Mater. 47 (1999) 2089-2108.
5. Benson, D.J., Tong, W., and Ravichandran, G., Modelling Simul Mater. Sci. Engr. 3 (1995) 771-796.
6. Eakins, D.E. and Thadhani, N.N., Acta Mater. 56 (2008) 1496-1510.
7. Bell, R.L., et al., *CTH Users Manual and Input Instructions*, V 7.1, Sandia National Laboratories, New Mexico, 2006.
8. Taylor, P.A., *CTH Reference Manual: The Steinberg-Guinan-Lund Viscoplastic Model*, Sandia National Laboratories, New Mexico, 1992.
9. Shankar, M.R., et al., Acta Mater. 53(2005) 4781-4793.
10. Meyers, M.A., *Dynamic Behavior of Materials*, John Wiley & Sons Inc., New York, 1994.